Applied Mechanics and Materials Vol. 660 (2014) pp 836-840
© (2014) Trans Tech Publications, Switzerland
doi:10.4028/www.scientific.net/AMM.660.836

Submitted: 20.07.2014
Revised: 07.08.2014
Accepted: 12.08.2014

FEA-Based Design Study of 12-Slot 14-Pole Outer-Rotor Dual Excitation Flux Switching Machine for Direct Drive Electric Vehicle Applications

Md Zarafi Ahmad[1, a *], Erwan Sulaiman[1,b], Zainal Alam Haron[1,c], and Faisal Khan[2,d]

[1]Electrical Power Engineering Department, Universiti Tun Hussein Onn Malaysia (UTHM)

86400 Parit Raja, Batu Pahat, Johor Malaysia

[2]Department of Electrical Engineering, COMSATS Institute of Information Technology (CIIT), 22060 Abbottabad, KPK, Pakistan

[a]zarafi@uthm.edu.my, [b]erwan@uthm.edu.my, [c]zainalal@uthm.edu.my, and [d]faisalkhan@ciit.net.pk

Keywords: Outer-rotor, dual excitation, flux switching machine, direct drive, electric vehicle.

Abstract. This paper presents an investigation into feasibilities design of 12-Slot 14-Pole outer-rotor dual excitation flux switching machine (ORDEFSM) for direct drive electric vehicle (EV) applications. The stator of the proposed machine consists of iron core made of electromagnetic steels, armature coils, permanent magnet (PM) and field excitation coils (FECs). The FECs in this proposed machine is used as a secondary field mmf source to support the main flux source from PM. Therefore, the proposed machine has extra advantage of variable flux control capability as compared with the conventional flux switching machines (FSMs). The rotor is composed of only stack of iron and hence, it is robust and suitable for high speed operation. The design target for the maximum torque and power density, and the maximum speed are more than 333 Nm, 3.5 kW/kg, and 20,000 r/min, respectively. The results obtained from two-dimensional (2-D) FEA study show that the initial design of the proposed machine has achieved the maximum torque, power density and maximum speed of 244.76 Nm, 3.47 kW/kg, and 20,000 r/min, respectively. Thus, it is expected that the proposed machine potentially to achieve the target performances by implementing optimization process using deterministic optimization method.

Introduction

Nowadays, growth of vehicles transportation has increased rapidly all over the world. Even the growths have brought benefits to many things; it also has contributed for global warming due to the emission of carbon dioxide (CO_2). According to a report in 2008 that has been reported in United State of America (USA), the major source of CO_2 emission is come from conventional internal combustion engine (ICE) vehicles, which contributes up to seven percent in 2000. The phenomenon is keep rising and expected to be doubled by 2050 [1]. Due to these concerns, a lot of government agencies, institutions, and private organization have developed more stringent standards for fuel consumption and vehicles emissions. Thus, the most appropriate solution in reducing greenhouse effect is by transforming the use of ICE with electric base vehicle. Hence, since a decade ago electric, hybrid, and fuel-cell vehicles are among the attractive research topic with the aim to reduce the vehicles emissions.

In the development of electric vehicle (EV), electric motor is among of the essential part to be considered for drive purposes. As well known, the electric motor use for heavy application such as in aerospace and automotive applications, it is essential to have high torque and power density capability [2]. Previously, permanent magnet (PM) brushless machines are widely used for many applications due to their advantages of high torque capability. Nevertheless, due to the PMs are located on the rotor, the machines are suffer from demagnetization effects which resulting in eddy current loss in the rotor. The main reason on this issue is difficulty to manage the temperature on the rotor.

In recent years, flux-switching motors (FSMs) have been extensively investigated due to their several advantages of robust rotor structure, higher torque density, and efficiency. With all excitation components located on the stator, the temperature rise of the machine can easily managed. The FSMs have been used in many applications ranging from wind power generation, automotive, aerospace, power tools and etc [3-5]. There are three type of FSMs and can be classified into permanent magnet (PM) FSMs, hybrid excitation (HE) FSMs, and field excitation (FE) FSMs. Both PMFSMs and FEFSMs have only single excitation flux source either come from PM or FE coil, while in HEFSM the magnetic flux source is generated from PM and FECs [6].

However, most of research have been reported are mainly focused on inner-rotor configuration [7-9] and difficult to find the outer-rotor FSM. Lately, a PMFSM has been first introduced for light traction EV applications [10-11]. Nonetheless, with single magnetic flux source of constant PM, it also may suffer from demagnetization effect. Thus, this paper presents a design study on 12S-14P outer-rotor hybrid excitation flux switching machine (HEFSM) to meet the requirement of in-wheel drive electric vehicle (EV). Based on 2-D analysis demonstrated, the machine has ability to achieve high torque and power density and suitable to be applied for EV drive system

12S-14P Outer-Rotor HEFSM Design Restrictions and Specifications

The design restrictions and specifications of the proposed outer-rotor HEFSM are similar with the interior permanent magnet synchronous machine (IPMSM) installed in Toyota Lexus RX400h [12]. With the PM volume reduced to 1.0 kg, 333 Nm and 123 kW is the target for maximum torque and power, respectively. Besides, the maximum voltage and current of the inverter is set at 650 V, and 360 Arms, respectively. Furthermore, both of the maximum armature current and field excitation current density is set to 30 A/mm^2. Finally, with the target weight of the machine is 30 kg, thus the proposed machine will having a torque and power density of 11.1 Nm/kg, and 4.1 kW/kg, respectively. In this study, the slot area of armature coil and field excitation coil is calculated using equation (1) and (2).

$$S_a = \frac{I_a N_a}{\alpha J_a} \tag{1}$$

$$S_e = \frac{I_e N_e}{\alpha J_e} \tag{2}$$

From Eqn. (1) and (2), α is the filling factor, while I_a and I_e are rated armature current and FEC current, respectively. N_a and N_e is the number of turn of armature coil and field excitation coil.

Open Circuit Analysis

Armature Coil Arrangement Test of PM Flux. The first step of designing machine is to examine the armature coil phase and polarity on each of armature coil slot. In conjunction with this aim, the coil arrangement test is implemented to confirm the principle operation of the proposed outer-rotor HEFSM. Initially, the polarity of all the armature coils are set in counter clockwise direction, while the DC FEC and PM polarities are set in alternate direction in order to provide 12 north and 12 south poles, respectively. Hence, based on a balance three phase system, the three phase of 12 armature coils are determined by observing and analyzing the magnetic flux linkage on each of armature coil. On the other hand, the armature current density, J_a and DC FEC current density, J_e is set to 0 A/mm^2, in which the flux is generated from PM only. From the coil arrangement test, it is found that the armature coils labeled as C1, C4, C7 and C10 represent the V-flux, while the armature coils labeled as C2, C5, C8, and C11 represent the U-flux, and armature coils labeled as C3, C6, C9, and C12 represent for W-flux of the machine as shown in Fig. 1. Once the polarity and phase of each armature coil has been identified, the three-phase fluxes are plotted as shown in Fig. 2. From the figure, it can be seen that the maximum amplitude of generated flux is approximately 0.011 Wb with solidly sinusoidal waveform. Therefore, the three-phase system of the

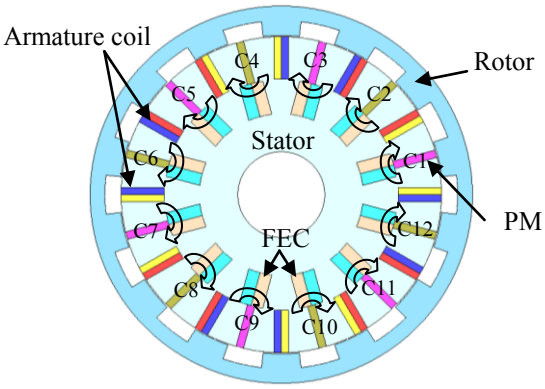

Fig. 1 Armature coil phase setting

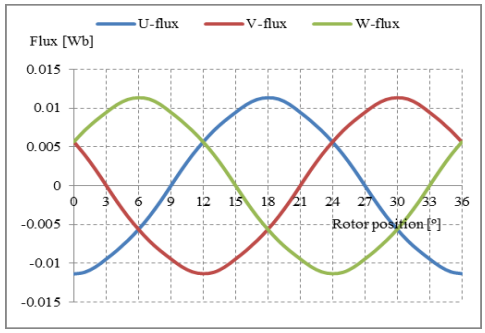

Fig. 2 Three-phase flux linkage produced by PM

proposed machine were identified and its principle operation has been proved through a coil arrangement test.

PM Flux Distribution. The open circuit field distribution of PM is also investigated as shown in Fig 3. It shows that the flux at rotor pole 1 (P1) flows from stator to the rotor and return through rotor pole 2 (P2) making a complete one flux cycle. It is obvious that, 50% of the PM flux flows from stator to rotor while the remaining flux flows around the DC FEC slot to form a complete 12 cycles of flux. However, very high flux density occurs between the adjacent of FEC slot and between the lower edge of armature coil and upper edge of DC FEC slots which results in flux saturation. Therefore, the appropriate distance between them needs to be examined to minimize the flux saturation effect.

Cogging Torque. The cogging torque of the proposed machine in open circuit condition is illustrated in Fig. 4. It is observed in 36º of rotor position which is one electric cycle. From the figure, it is clearly shown that the cogging torque is considered low with the maximum peak-to-peak is approximately 10.69 Nm. Thus, the cogging torque has ability to be reduced by conducting design optimization and improvement of the motor especially on the distance of armature coil and DC FEC slot.

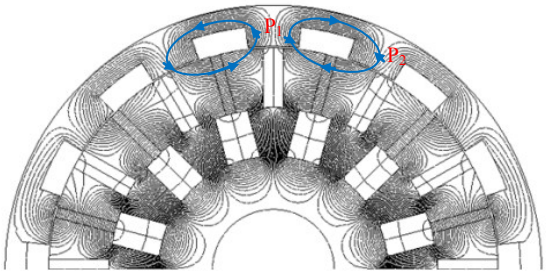

Fig. 3 Open circuit field distribution of the proposed motor

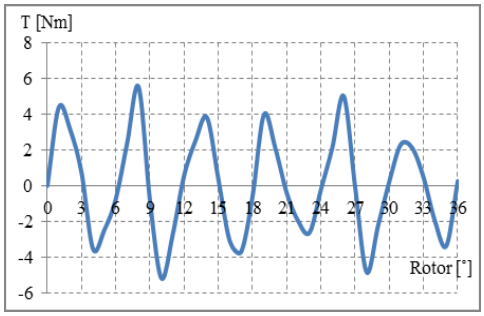

Fig. 4 Cogging torque of the proposed motor

Flux Characteristics at Various Current Densities. The flux linkage of PM and various DC FEC current densities are demonstrated in Fig. 5. It is obvious that when DC FEC current density, J_e start increased, the flux linkage also increasing and reach to maximum when J_e set to 10 A/mm^2. The maximum flux linkage at this condition is approximately 0.051 Wb which is increased more than three times when compared with flux linkage come from PM only. When further increased of J_e, the flux linkage starts to reduce and finally when J_e is set to maximum of 30 A/mm^2, the magnitude of flux linkage is approximately 0.028 Wb. This phenomenon is expected due to flux saturation when higher J_e is injected to the system beyond 10 A/mm^2. However, this analysis has proved that the additional DC FEC can improve the generated flux from PM and offers variable flux control capability.

Short Circuit Analysis

Magnetic Flux and Instantaneous Torque Characteristic. The generated magnetic flux from individual active parts namely PM, DC FEC and armature coil are also investigated and analyzed. In short circuit analysis the DC FEC is set to maximum current density of 30 A/mm^2 while for the armature coil is also set to it maximum current density of 30 A_{rms}/mm^2. At the condition of DC FEC and armature coil only, the PM need to be set as an air. The comparison of the individual flux generated from PM, DC FEC and armature coil are plotted in Fig. 6. The flux from individual PM, DC FEC and armature coil are highlighted in blue, red, and green color, respectively. Thus, when all components are set at maximum, the resulting flux is shown in dotted line. From the flux line result, it is clearly shown that the amplitude obtained is 0.066 Wb with the output torque and power of 237.35 Nm and 94.80 kW, respectively. Consequently, the instantaneous torque waveform of the proposed motor at maximum current density is illustrated in Fig. 7. From the figure, the peak-to-peak torque is approximately 60.9 Nm. The peak-to-peak torque is considerably high that may result in high vibration and noise; therefore design improvement should be conducted to reduce it into the acceptable range.

Torque Characteristic at Various Current Densities. The torque characteristics at various armature current density and DC FEC current density are also investigated. The results obtained is plotted in Fig. 8, in which the armature coil and DC FEC current densities are varied from 0 to 30 A/mm^2.

The graph show that the maximum torque of 243.52 Nm of initial design machine is obtained when armature and FEC current densities are set to 30 A_{rms}/mm^2 and 25 A/mm^2, respectively, whereas the maximum power obtained at the speed of 3000 rpm is 83.03 kW. These results indicate that the torque and power of the machine can be controlled by varying the current densities of DC FEC and armature coil.

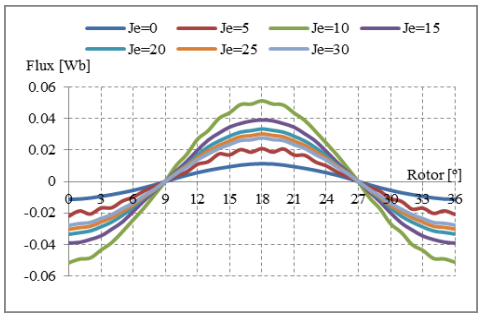

Fig. 5 Flux linkage at various DC FEC current densities

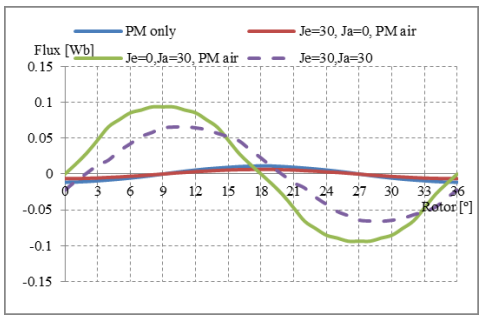

Fig. 6 Flux generated from PM, DC FEC and armature coil

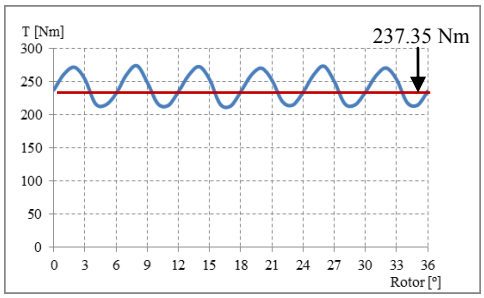

Fig. 7 Instantaneous torque characteristic

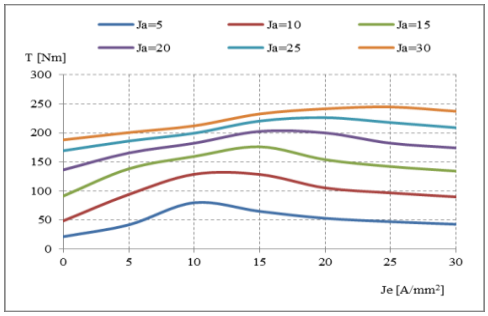

Fig. 8 Torque versus FEC current dentisy at various armature current density

Conclusion

In this paper, design investigation of 12-Slot 14-Pole outer-rotor dual excitation flux switching machine has been presented. The three phase armature coil and its polarity of the proposed machine have been examined through the coil arrangement test analysis. The proposed machine has rugged rotor structure which is designed without any PM or winding on the rotor core, thus suitable for high speed condition. Lastly, based on the investigation results have obtained, the target performances of the proposed machine can be achieved by conducting design refinement and optimization to improve the flux flow from stator to the rotor.

References

[1] The King Review of low-carbon cars of low-carbon cars - Part II: recommendations for action, (2008). Available at: www.hm-treasury.gov.uk/king

[2] Z. Q. Zhu and D. Howe, Electrical machines and drives for electric, hybrid, and fuel cell vehicles, Proc. IEEE, vol.95, no. 4, (2007) pp. 746-765, 2007.

[3] Y. Amara, E. Hoang, M. Gabsi, and M. Lecrivain, Design and comparison of different flux-switching synchronous machines for an aircraft oil breather application, Euro. Trans Electr. Power, no. 15, (2005) pp. 497-511.

[4] C. Pollock, H. Pollock, R. Borron, J. R. Coles, D. Moule, A. Court, and R. Sutton, Flux-switching motors for automotive applications, IEEE Trans. Ind. Appl., vol. 42, no. 5, (2006) pp. 1177-1184.

[5] M. J. Jin et al, Cogging torque suppression in a permanent magnet flux-switching integrated starter generator, IET Electric Power Appl., vol 4, no. 8, (2010) pp. 647-656.

[6] E. Sulaiman, T. Kosaka, and N Matsui, High power density design of 6slot-8pole hybrid excitation flux switching machine for hybris electric vehicles, IEEE Trans. on Magn. vol.47, no. 10, (2011) pp.4453-4456.

[7] J.T. Chen and Z.Q. Zhu, Winding configuration and optimal stator rotor pole combination of flux-switching PM brushless machines, IEEE Trans. on Energy Conversion, vol. 25, (2010) pp. 293-302.

[8] Y. Wang and Z. Deng, Comparison of hybrid excitation topologies for flux-switching machines, IEEE Trans. on Magn., vol. 48, no. 9, (2012)

[9] Y. Tang, J.J.H. Paulides, T.E. Motoasca, and E.A. Lomonova, Flux-switching machine with DC excitation, IEEE Trans. on Magn., vol. 48, no. 11, (2012).

[10] Y. Wang, M.J. Jin, J. Shen, W.Z. Fei, and P.C.K. Luk, An outer-rotor permanent magnet flux-switching machine for traction application, Energy Conversion Congress and Expo-sition (ECCE), (2010) pp. 1723-1730.

[11] W. Fei, P. Chi, K. Luk, S. Member, J. X. Shen, Y. Wang, and M. Jin, A Novel Permanent-Magnet Flux Switching Machine With an Outer-Rotor Configuration for In-Wheel Light Traction Applications, IEEE Transactions on Industry Applications, vol. 48, no. 5, (2012) pp. 1496–1506.

[12] E. Sulaiman, T. Kosaka, N. Matsui, and M. Z. Ahmad, Design Studies on High Torque and High Power Density Hybrid Excitation Flux Switching Synchronous Motor for HEV Applications, in IEEE International Power Engineering and Optimization Conference (PEOCO), (2012) pp. 333–338.